Enhanced Gene Delivery Triggered by Dual pH/Redox Responsive Host-Guest Dimerization of Cyclooligosaccharide Star Polycations

Ana I. Carbajo-Gordillo, José López-Fernández, Juan M. Benito, José L. Jiménez Blanco, María L. Santana-Armas, Gema Marcelo, Christophe Di Giorgio, Cédric Przybylski, Carmen Ortiz Mellet,* Conchita Tros de Ilarduya,* Francisco Mendicuti,* and José M. García Fernández*

A robust strategy is reported to build perfectly monodisperse star polycations combining a trehalose-based cyclooligosaccharide (cyclotrehalan, CT) central core onto which oligoethyleneimine radial arms are installed. The architectural perfection of the compounds is demonstrated by a variety of physicochemical techniques, including NMR, MS, DLS, TEM, and GPC. Key to the strategy is the possibility of customizing the cavity size of the macrocyclic platform to enable/prevent the inclusion of adamantane motifs. These properties can be taken into advantage to implement sequential levels of stimuli responsiveness by combining computational design, precision chemistry and programmed host-guest interactions. Specifically, it is shown that supramolecular dimers implying a trimeric CT-tetraethyleneimine star polycation and purposely designed bis-adamantane guests are preorganized to efficiently complex plasmid DNA (pDNA) into transfection-competent nanocomplexes. The stability of the dimer species is responsive to the protonation state of the cationic clusters, resulting in dissociation at acidic pH. This process facilitates endosomal escape, but reassembling can take place in the cytosol then handicapping pDNA nuclear import. By equipping the ditopic guest with a redox-sensitive disulfide group, recapturing phenomena are prevented, resulting in drastically improved transfection efficiencies both in vivo and in vitro.

1. Introduction

Viruses cunningly achieve their own transport and target infection by subverting the delicate cellular structure of the host cell and its signal transduction pathways. Infection and propagation cycles are accomplished through concerted multi-step processes comprising hierarchical self-assembly, defined tropism, specific cellular binding and uptake, and opportune uncoating. All of these phases are well-programmed and tightly regulated in time and space, involving dynamic conformational changes and alterations in supramolecular interactions that are precisely triggered by signals emanating from the microenvironment. Nonviral vectors (such as cationic lipids and polymers) exhibit superior safety and biocompatibility, but have enhanced difficulty in overcoming biological barriers while keeping the virus extraordinary infectivity potential, given their lack of corresponding biological characteristics.[1] In the last years, a variety of intelligent supramolecular systems

A. I. Carbajo-Gordillo, J. López-Fernández, J. M. Benito, J. M. García Fernández
Instituto de Investigaciones Químicas (IIQ)
C/ Américo Vespucio 49, Sevilla 41092, Spain
E-mail: jogarcia@iiq.csic.es

J. L. Jiménez Blanco, C. Ortiz Mellet
Department of Organic Chemistry
Faculty of Chemistry
University of Seville
C/ Profesor García González 1, Seville 41012, Spain
E-mail: mellet@us.es

M. L. Santana-Armas, C. Tros de Ilarduya
Department of Pharmaceutical Technology and Chemistry, School of Pharmacy and Nutrition
University of Navarra
Pamplona 31080, Spain
E-mail: ctros@unav.es

The ORCID identification number(s) for the author(s) of this article can be found under https://doi.org/10.1002/marc.202200145

superimposing different levels of organizations and environmental stimuli responsiveness, based on host-guest complex formation, have been proposed to overcome this critical bottleneck.[2] A number of multifunctional materials have been fabricated based on this concept, including virus-mimicking architectures with good biocompatibility and transfection properties. Most reports regard polyformulations and nanocomposites entailing macromolecular components equipped with macrocyclic hosts, such as cyclodextrins (CDs),[3] cucurbit[n]urils,[4] calixarenes[5] or pillarenes,[6] and complementary guest motifs. In the presence of the nucleic acid partner, "'programmed packaging'" takes place to produce virus-like particles. The versatility of host-guest events then allows presetting the system to undergo a shift from preferential guest inclusion to dissociation, or vice versa, thus affecting the topology, internal structure, and/or stability of the whole supramolecular edifice in response to specific cues such as changes in pH, redox potential, or levels of reactive species or enzymes.

A residual limitation is the polydisperse character of the vector components: differently from virus capsids, which are made of one or a few perfectly defined proteins, conformationally indefinite constituents and/or polymeric materials are most often found in artificial virus emulators. Nanosized molecular entities (molecular nanoparticles, MNPs[7]) represent an interesting alternative.[8] MNP platforms can be finely tuned to encode precise supramolecular behaviors, offering unprecedented architectural versatility.[9] Most reports in this category focus on polycationic CDs and exploit their unique inclusion capabilities.[10] Interestingly, bridging two molecules of the CD vector with appropriate spacers affords a new entity with distinctly different capacities of interacting with nucleic acid partners, which has been found to strongly impact the topological properties of the resulting nanocondensates and their in vivo tropism.[11] Since the stability of supramolecularly connected polycationic dimers is pH-dependent, this strategy represents a unique opportunity to impart stimuli sensitiveness and organ targeting while preserving vector monodispersity, with no additional synthetic cost.

We recently reported that macrocycles built from the disaccharide α,α'-trehalose (cyclotrehalans, CTs) represent an appealing alternative to CDs.[12] Differently from CDs, CTs depict a convex inner hydrophobic cavity flanked by secondary hydroxyls that project from concave faces.[13] In principle, this architecture must facilitate the access of size-fitting guests to the cavity even if relatively bulky O-substituents are present. We hypothesized that these favorable characteristics could be exploited to access non-viral vectors warranting efficient pDNA complexation and timely release by judiciously customizing the host and guest partners.
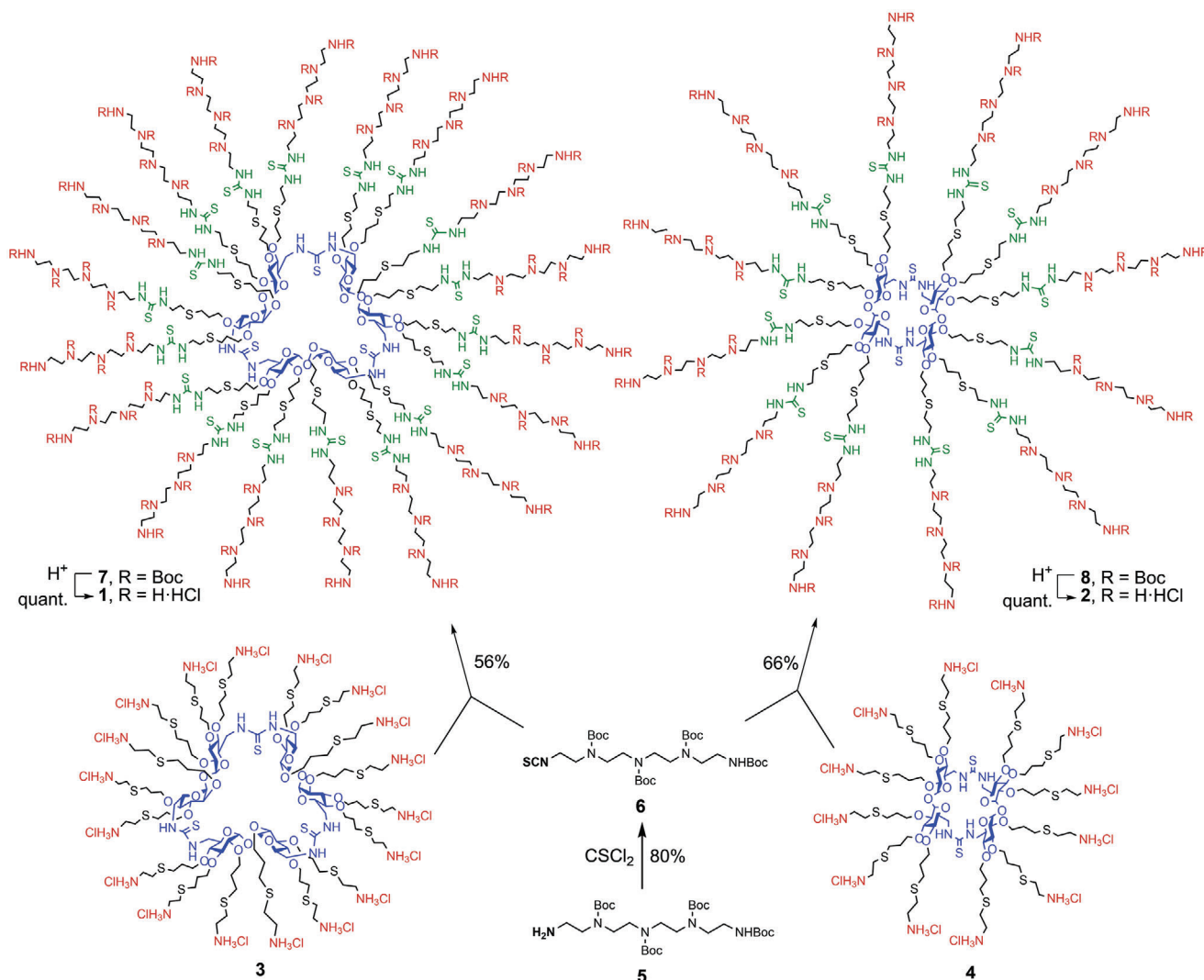
2. Results and Discussion

Based on previous results proving the benefit of multicharged oligoethyleneimine (OEI) cationic heads in MNP vector design,[14] we devised star-shape prototypes bearing tetraethyleneimine (TEI) appendages stretching out from a trimeric (CT3) or dimeric (CT2) platform, namely compounds **1** and **2** (**Scheme 1**). Their preparation was accomplished in two steps from the respective cysteaminylated CT3 and CT2 precursors **3** and **4** by click-type thiourea-forming reaction[15] with the Boc-protected isothiocyanate-armed TEI derivative **6**, accessible by isothiocyanation of the corresponding amine **5**[14b] with thiophosgene, followed by cleavage of the carbamate protecting groups. Of note, all the coupling steps leading from commercial α,α'-trehalose to the target star polycations are highly efficient and metal catalyst-free, which represents an important advantage for biological applications.

Structural perfection and sample homogeneity of compounds **1** and **2** was initially gauged by ^{1}H and ^{13}C NMR. Although fully compatible with the proposed structure, extensive line broadening consequence of slow rotation about the N–C(= S) thiourea bonds made it problematic to warrant diastereomeric purity, as seen in Figures S3 and S5, Supporting Information).[16] The Boc-protected precursors **7** and **8** afforded pseudomelecular ions in accordance with the expected molecular weight by electrospray ionization (ESI) mass spectrometry and correct combustion analysis data. The corresponding pseudomolecular ions of the unprotected compounds **1** and **2** were not observed, however, because their numerous thiourea and amine groups severely thwart ionization.[17] An alternative strategy, consisting of the preformation of noncovalent complexes with a single-stranded 12-mer DNA (5-AAGCCCGCCCAA-3; DNAi),[18] let observe the MALDI-TOF pseudomolecular ion peaks corresponding to the theoretical masses (Figure S8 and S9, Supporting Information). Molecular weights determined by gel permeation chromatography further agreed well with the calculated values (**Figure 1**A), whereas the very low polydispersity (PD) data, close to unity, supported structural uniformity. Dynamic light scattering (DLS) of aqueous solutions of **1** and **2** showed unimodal populations of particles with hydrodynamic diameters (D_h values) close to 5.7 and 5.4 nm, in reasonable agreement with computational estimates (3.35 and 3.17 nm), and positive ζ-potential values for both **1** and **2** (Figure 1B), anticipating that the primary amine groups are protonated to a large extent at pH close to neutrality. It is worth pointing out that there is often a discrepancy between TEM and DLS particle size determinations that is attributed to factors associated with the high vacuum conditions of TEM and the hydrodynamic and electrokinetic effects operative in DLS measurements.[19] The same applies to sizes estimation divergences between computed structures and DLS.

The CT3 macroring depicts a permanent cavity averaging 7.1 Å internal diameter, close to that of βCD (7.8 Å), that can host lipophilic guest molecules of compatible size. Its

G. Marcelo, F. Mendicuti
Department of Analytical Chemistry
Physical Chemistry and Chemical Engineering
Faculty of Chemistry
University of Alcalá
Alcalá de Henares, Madrid Spain
E-mail: francisco.mendicuti@uah.es

C. Di Giorgio
Institut de Chimie Nice
UMR 7272
Université Côte d'Azur
28, Avenue de Valrose, Nice F-06108, France

C. Przybylski
Institut Parisien de Chimie Moléculaire (IPCM)
CNRS
Sorbonne Université
Paris France

**ADVANCED
SCIENCE NEWS**

www.advancedsciencenews.com

{M} acro-
molecular
Rapid Communications

www.mrc-journal.de

Scheme 1. Synthesis of the star-shaped polycationic cyclotrehalans **1** and **2**.

ternary symmetry and dimensions are ideally suited for the inclusion of adamantane motifs (**Figure 2**).[20] Computational models suggested that the ditopic guests **bisAd** (see Scheme S2, Supporting Information, for details on the synthesis) and **SS-bisAd**, having 36-single-bond connectors, could avoid steric clashes upon bridging two molecules of **1**, thus allowing the assemblage of supramolecular dimers preorganized for optimally bridging quasi-parallel segments of DNA chains. The general simulation protocol implemented to get a deeper insight into the interactions that govern the hierarchical process that leads to the formation of ternary nanocomplexes with pDNA (CTplexes) is depicted in **Figure 3** for the **(1)₂/SS-bisAd** supramolecular dimer. First, the stability of the dimer was studied by molecular mechanics (MM) in explicit water. The minimum binding energy (MBE) structure was initially obtained by sequentially approaching two molecules of **1**, in the corresponding perhydrochloride form, with their center of mass on the γ axis in a coordinate system (Figure 3A). It corresponded to a structure in which the adamantane moieties are deeply inserted in the CT3 cavity. The MBE structure,

after removing the chloride anions, was then placed between two symmetrically located and oriented B DNA helix fragments containing twenty nucleotides (CGCGAATTCGCGAATTCGCT), and the oligonucleotide chains were approached simultaneously in steps of 1 Å (**Figure 3**B). The binding energies obtained using this procedure, which were rather favorable, led to efficient packing, especially when the DNA fragments approached the supramolecular dimer with their helical axes parallel to the **bisAd** or **SS-bisAd** chain, so-called lateral approaching (Figure 3C; see also the Supporting Information for full computational details).

Predictably, the stability of the corresponding CTplexes will depend on the degree of protonation of the cationic arms: upon cell uptake and acidification of the endosome, electrostatic repulsions would promote the dissociation of the dimer species. The supramolecular amphiphile thus formed then can interact with the endosome membrane and facilitate endosomal scape. Once in the cytoplasm (pH 7) re-assembly of the **(1)₂/bisAd**/pDNA nanocomplexes can ensue, hampering pDNA import into the nucleus. In the case of **SS-bisAd**, however, the high

	1	**2**
Mw_{theor}	7458	4948
Mn_{GPC}	7506	4962
PD	1.02	1.01

DLS data

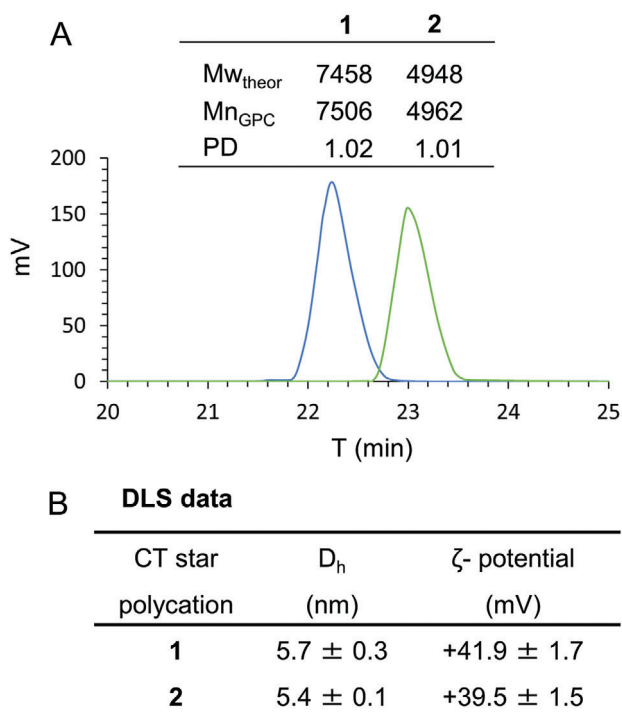| CT star polycation	D_h (nm)	ζ- potential (mV)
1	5.7 ± 0.3	$+41.9 \pm 1.7$
2	5.4 ± 0.1	$+39.5 \pm 1.5$

Figure 1. A) GPC-RI traces of the CT3 and CT2 star polycations **1** and **2**, respectively, with an indication of the molecular weights calculated from the structure (Mw_{theor}), or measured by GPC (Mn_{GPC}, number-average) and the polydispersity (PD); the elution time decreases with the Mw. B) Hydrodynamic diameter and ζ-potential data (DLS).
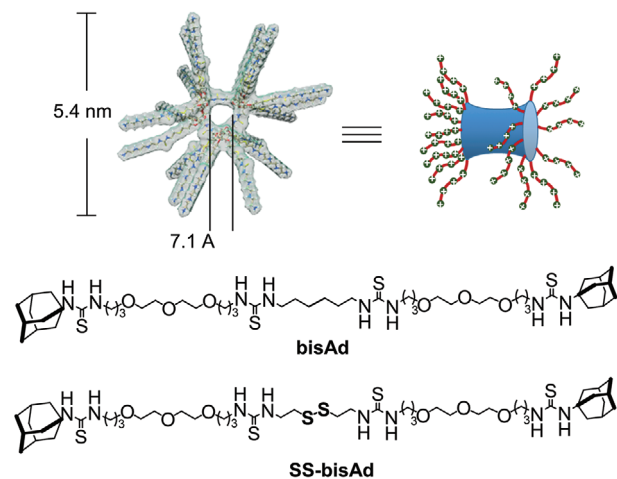

Figure 2. 3D Structure of **1**, cartoon illustrating its concave/convex topology and structures of the ditopic **bisAd** and **SS-bisAd** guests.

Figure 3. A) Coordinate system used for two molecules of **1** (MBE structure) approaching a molecule of **SS-bisAd** in the most favorable **1**-to-**SS-bisAd** relative orientation. B) The coordinate system used for two DNA fragments approaching the MBE structure of the ($1)_2$/**SS-bisAd** supramolecular dimer along the y coordinate (lateral approaching). C) 3D molecular model of the ($1)_2$/**S-S-bisAd** (MBE) and schematic representation of the interactions with two DNA segments after lateral approaching.

concentration of glutathione (GSH) in the cytosol would promote disulfide bridge cleavage, thereby deactivating the vector for strong pDNA recapture. This is critical for enabling subsequent nuclear entry of pDNA: although some examples have demonstrated the presence of cationic polymer molecules in the nucleus during polyplex-mediated transfection,[21] the current evidence supports that pDNA must be essentially free or loosely bound to undergo either integration into the nucleus during nuclear envelop re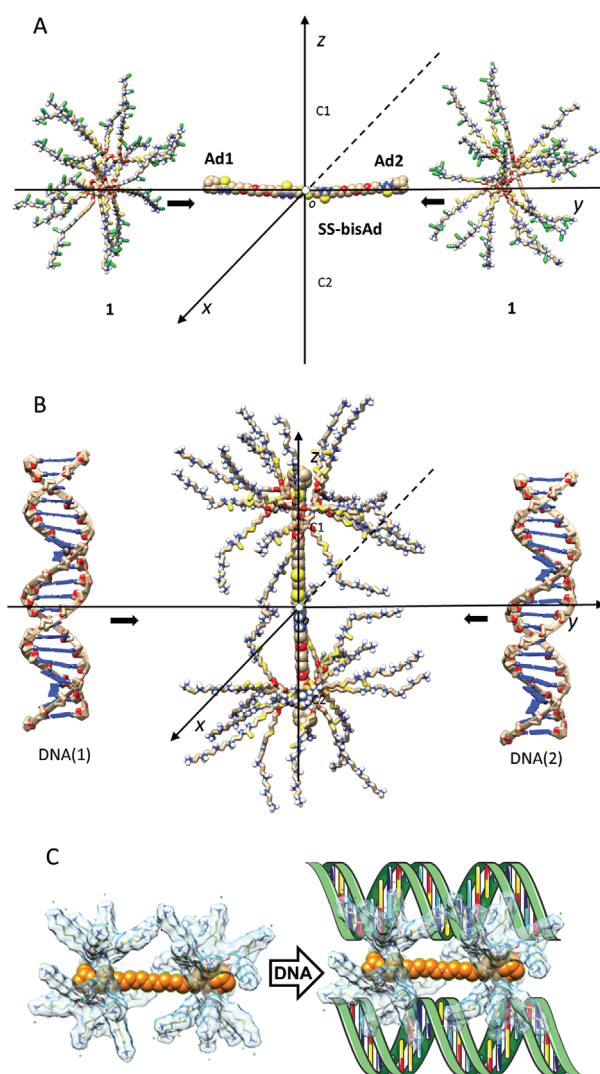formation at telophase in dividing cells[22] or, eventually, active import through the nuclear pore complex[23] (**Figure 4**). In CT2 derivatives the cavity is collapsed;[24] dissimilarities in pDNA complexation and transfecting properties between **1** and **2** in combination with the ditopic adamantane derivatives should then be principally ascribed to the host-guest component of the process.

The capabilities of **1** and **2** to form stable nanocomplexes (CTplexes) with pDNA (luciferase-encoding pCMV-LucVR1216) were initially verified at protonable nitrogen/phosphorus (N/P) ratios 5, 10, and 20 in 4-(2-hydroxyethyl)-1-piperazineethanesulfonic acid (HEPES) buffer (pH 7.4, 10 mM). DLS (**Table 1**) evidenced the formation of self-assembled nanoparticles, with positive ζ-potentials in the range 17–24 mV. The particle average hydrodynamic diameter

**ADVANCED
SCIENCE NEWS**
www.advancedsciencenews.com

Macro-
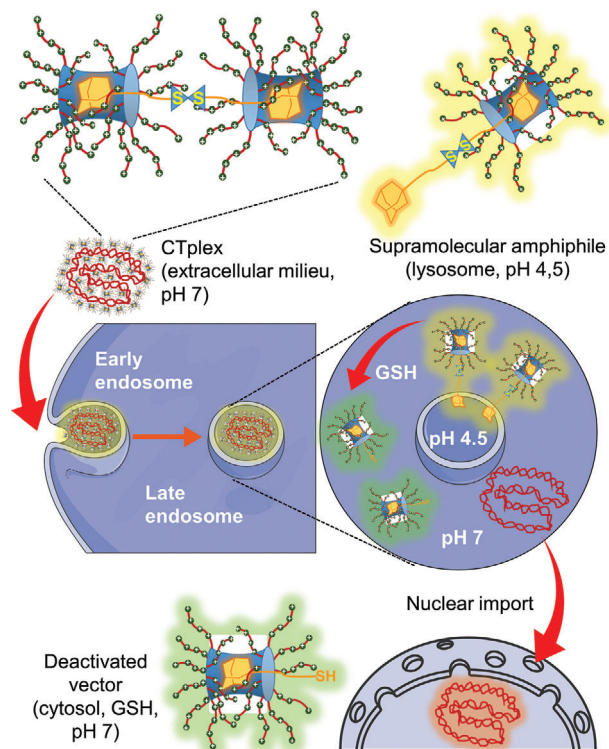molecular
Rapid Communications
www.mrc-journal.de

Figure 4. Representation of the processes involved in pDNA complexation and release using the proposed dual pH/redox-responsive strategy: the preorganized dimer efficiently condenses pDNA into nanocomplexes (CTplexes) at pH 7 that undergo cell uptake. Upon acidification at the lysosome, the dimer dissociates and endosomal escape, promoted by the resulting supramolecular amphiphile, takes place. The high concentration of glutathione in the cytosol then brakes the S–S bridge in the **SS-bisAd** guest, preventing pDNA recapture. The loosely bound pDNA can then be incorporated into the nucleus during cell division or, to a lesser extent, by active import through the nuclear pore complex.

(D_h) values were found to be very similar in the two series, decreasing from 155–149 nm at N/P 5 to 138–132 nm at N/P 10 and 107–105 nm at N/P 20 (Table 1). This is significantly higher as compared with D_h values previously observed for other cyclooligosaccharide-based gene carriers (50–80 nm).[25] DNA protection and integrity in the formulations were confirmed by electrophoresis mobility shift assay (EMSA) in 0.8% agarose gel, with staining by the intercalating agent ethidium bromide. As a compromise, N/P 10 formulations were selected for further

studies (**Figure 5**A,B, respectively). In accordance with DLS data, TEM micrographs showed multiglobular aggregates analogous to those frequently observed for polycationic dendrimer vectors such as the poly(amidoamine) (PAMAM) dendrimers (Figure 5C,D).[26] Interestingly, the topological properties of the CTplexes obtained from **1** conspicuously changed upon preincubation with **bisAd** or **SS-bisAd**: small particles (D_h, 70–50 nm) with higher ζ-potentials (32–36 mV; Table 1 and Figure 5E,F) were obtained under identical conditions. The TEM images confirmed the small size of the CTplex formulations. Compacted globules with mean apparent diameters of about 40 nm were observed in the micrographs, pointing out to their pDNA monomolecular character.[27] Sharply differently, no alterations were detected in the case of the CT2 homolog **2**, strongly suggesting that the observed transformations arise from host-guest driven reinforcement of the interactions of **1** with pDNA chains. Remarkably, when the $(1)_2$/**bisAd**/pDNA or $(1)_2$/**SS-bisAd**/pDNA CTplexes were formulated at pH 4.5 considerably larger objects, probably involving supramolecular amphiphile aggregates, were found both by TEM (Figure 5G,H) and DLS (Figure 5I,J), in agreement with the presumed weakening of the interactions holding the supramolecular dimers consequent to an increase in the protonation of the cationic clusters. Further on, when incubating $(1)_2$/**SS-bisAd**/pDNA CTplexes in water solution containing 10 mM GSH, a scenario that mimics the GSH concentration in the cytosol, an increase in D_h was observed with time. After four hours, the particle size was about 850 nm hydrodynamic diameter (Figure 5J). This is indicative of disruption of the nanocomplex structure and swelling following reduction of the disulfide bonds, confirming the redox responsiveness of the system. As expected, a parallel experiment using $(1)_2$/**bisAd**/pDNA CTplexes revealed no change in particle size.

The impact of guest-promoted supramolecular preorganization of **1** in in vitro transfection efficiency was tested in African green monkey epithelial kidney COS-7, human hepatocellular carcinoma HepG2, human cervical carcinoma HeLa, murine embryonic hepatocyte BNL-CL2 and macrophage RAW 264.7 cells. Polyplexes generated from branched polyethyleneimine (bPEI, MW = 25 kDa) and lipoplexes formulated with lipofectamine 3000® (LP) were included as controls. For the sake of clarity, the data have been normalized to the value obtained for **1**/pDNA CTplexes in each cell line (**Figure 6**A; absolute values of luciferase expression are provided in the Supporting Information, Figure S20). Notably, this formulation already outperformed bPEI polyplexes and rivalled Lipofectamine 3000 performance in all cases.

Table 1. Hydrodynamic diameters and ζ-potentials (DLS) for the nanoplexes formulated with the CT star polycations **1** and **2** and pDNA (pCMV-Luc VR1216) at N/P 5, 10, and 20. Data obtained for the ternary formulations **1**/bisAd/pDNA and **1**/SS-bisAd/pDNA are also shown. Analogous formulations with compound **2** did not show any change or showed the presence of insoluble **bisAd** or **SS-bisAd** component.

CT star polycation	N/P 5		N/P 10		N/P 20	
	D_h [nm]	ζ- potential [mV]	D_h [nm]	ζ- potential [mV]	D_h [nm]	ζ- potential [mV]
1	149 ± 8	+18 ±5	122 ± 7	+25 ± 4	105 ± 4	+26 ± 3
2	155 ± 11	+17 ± 3	133 ± 6	+24 ± 3	107 ± 6	+25 ± 1
1/bisAd	70 ± 4	+33 ± 3	55 ± 3	+35 ± 2	50 ± 3	+36 ± 4
1/SS-bisAd	72 ± 5	+32 ± 4	58 ± 3	+34 ± 3	53 ± 3	+35 ± 3

ADVANCED SCIENCE NEWS
www.advancedsciencenews.com

[M] acro-
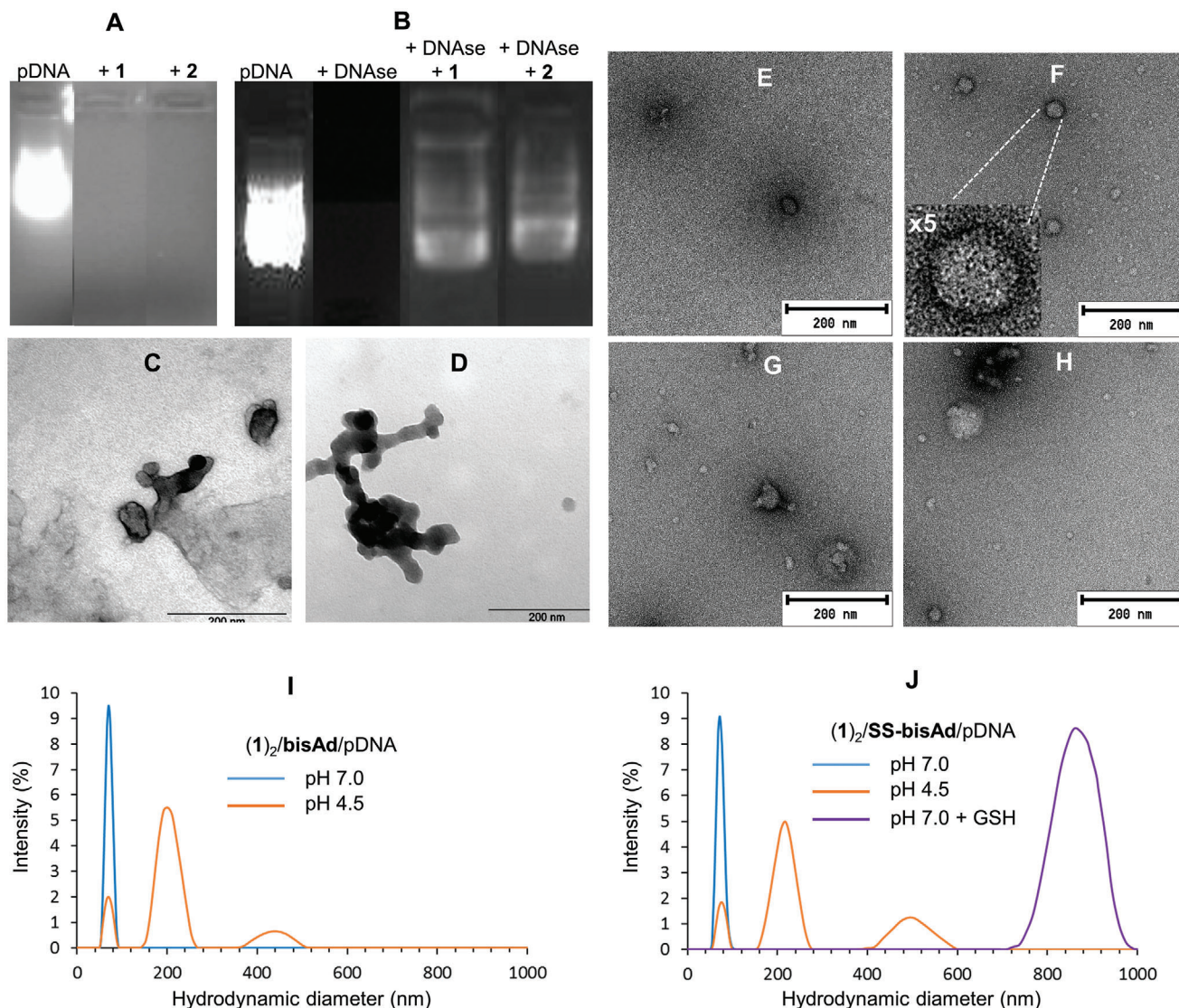molecular
Rapid Communications
www.mrc-journal.de

Figure 5. A,B) EMSA gels for nanocomplexes formulated with pDNA (pCMV-Luc VR1216) and the CT3 (**1**) and CT2 (**2**) star polycations at N/P 10, before (A) and after treatment with DNase I and subsequent dissociation of the complexes with sodium dodecylsulfate (B); Naked pDNA was used as a control. C,D) Representative TEM micrographs of the nanocomplexes obtained from **1** and **2**, respectively, upon formulation with the same pDNA at N/P 10 at pH 7. E–H) Representative TEM micrographs of (**1**)$_2$/**bisAd**/pDNA and (**1**)$_2$/**SS-bisAd**/pDNA nanocomplexes formulated at N/P 10 at pH 7 (E and F, respectively) or pH 4.5 (G and H, respectively). I,J) DLS profiles of (**1**)$_2$/**bisAd**/pDNA (I) and (**1**)$_2$/**SS-bisAd**/pDNA (J) nanocomplexes formulated at N/P 10 at pH 7 or pH 4.5 and, for the latter, at pH 7 in the presence of 10 mM GSH after 6 h incubation time.

The incorporation of the **bisAd** component had a modest effect in luciferase expression, with increments going from 1.3 to 1.5-fold. The pDNA recapture effect at the close-to-neutral cytosolic pH probably counteracts the expected favorable influence of improving extracellular CTplex stability and acid-promoted lysosomal escape abilities. Gratifyingly, replacing **bisAd** by the redox-sensitive **SS-bisAd** ditopic guest boosted transfection efficiency by over one order of magnitude (20 to 50-fold), providing a proof of concept of the proposed dual pH/redox-sensitive host-guest approach. As a negative control, transfection efficiencies achieved with **2/pDNA** CTplexes were essentially unaltered after the incorporation of either **bisAd** or **SS-bisAd**. None of the CTplex formulations was toxic to the cells (>85% cell viability, see Figure S19 in

the Supporting Information). The repercussion of vector preorganization and programmed disassembly of the CTplexes in the transfection outcome was much more drastic in in vivo settings. Indeed, raw N/P 10 **1**/pDNA CTplexes afforded poor transgene expression levels 24 h after systemic administration to mice intravenously, transfection occurring almost exclusively in the lung with negligible luminescence detected in the other organs analyzed (liver, spleen, kidney, and heart). The three-component CTplexes formulated with **bisAd** or **SS-bisAd** afforded neatly enhanced transfection efficiencies, by over 1–2 orders of magnitude, with preferential transgene expression in the liver and the spleen in the first case and almost exclusively in the liver for the latter (Figure 6B).
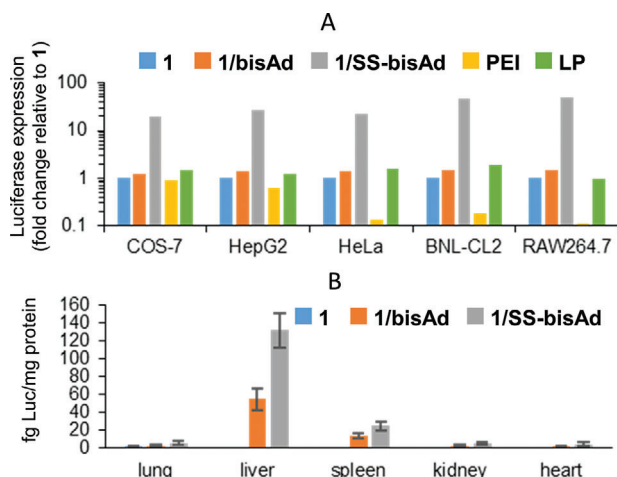
ADVANCED
SCIENCE NEWS
www.advancedsciencenews.com

{M}acro-
molecular
Rapid Communications
www.mrc-journal.de

Figure 6. A) Transfection efficiency in COS-7, HepG2, BNL-CL2, and RAW 246.7 cells for nanocomplexes formulated with **1**, **1/bisAd**, or **1/SS-bisAd** and the luciferase encoding gene pCMV-Luc VR1216 at N/P 10, in the presence of 10% fetal bovine serum (FBS). Data are normalized to the value obtained for **1**/pDNA CTplexes in each cell line; results for bPEI polyplexes and LP lipoplexes are included for comparison. B) Gene expression was conducted in vivo after intravenous administration of 60 µg of pCMV-Luc VR1216 using the above formulations. Bars represent the mean ± SD (n = 8 animals).

3. Conclusions

In conclusion, preorganization of a trehalose-based star polycation with inclusion capabilities by forming a host-guest dimer with a ditopic guest of appropriate length improves pDNA nanocomplexation abilities and concomitantly imparts pH responsiveness. The insertion of a disulfide bond in the guest connector further leads to a pH/redox responsive vector with significantly enhanced transfection efficiency. Importantly, the supramolecular species exhibit distinct in vivo tropisms. Thus, the organ destination can be modulated between the lung, spleen, and liver using the same star polycation, with no need of targeting ligand, which is remarkable. Differential nucleic acid delivery to different organs was previously realized with lipid nanoparticles (LNPs) by adjusting the N/P ratio or via the addition of supplemental molecules that modify the internal charge of the lipoplexes.[28] In our case, organ transfection profiles can be similarly tuned by promoting supramolecular dimerization of a perfectly defined molecular vector with a ditopic guest that, at the same time, imparts pH (for **bisAd**) or dual pH/redox responsiveness (for **SS-bisAd**), thus concomitantly enhancing transfection efficiency. Taken collectively, the results deliver a testable prototype to guide future host-guest based vector design.

Supporting Information

Supporting Information is available from the Wiley Online Library or from the author.

Conflict of Interest

The authors declare no conflict of interest.

Data Availability Statement

The data that support the findings of this study are available in the supplementary material of this article.

[1] a) N. Bono, F. Ponti, D. Mantovani, G. Candiani, *Pharmaceutics* **2020**, *12*, 183; b) I. Lostalé-Seijo, J. Montenegro, *Nat. Rev. Chem.* **2018**, *2*, 258; c) H. Yin, R. L. Kanasty, A. A. Eltoukhy, A. J. Vegas, J. R. Dorkin, D. G. Anderson, *Nat. Rev. Genet.* **2014**, *15*, 541.

[2] a) F.-Q. Li, Q.i-L. Yu, Y.-H. Liu, H.-J. Yu, Y. Chen, Y. Liu, *Chem. Commun.* **2020**, *56*, 3907; b) B. A. Badeau, C. A. Deforest, *Annu. Rev. Biomed. Eng.* **2019**, *21*, 241; c) A. S. Braegelman, M. J. Webber, *Theranostics* **2019**, *9*, 3017; d) C. Stoffelen, J. Huskens, *Small* **2016**, *12*, 96.

[3] a) H. Mousazadeh, Y. Pilehvar-Soltanahmadi, M. Dadashpour, N. Zarghami, *J. Controlled Release* **2021**, *330*, 1046; b) F. Seidi, Y. Jin, H. Xiao, *Carbohydr. Polym.* **2020**, *242*, 116277; c) Y.-M. Zhang, Y.-H. Liu, Y.u Liu, *Adv. Mater.* **2020**, *32*, 1806158; d) G. Rivero-Barbarroja, J. M. Benito, C. Ortiz Mellet, J. M. García Fernández, *Nanomaterials* **2020**, *10*, 2517; e) H. Cheng, X. Fan, C. Wu, X. Wang, L.i-J. Wang, X. J. Loh, Z. Li, Y.-L. Wu, *Macromol. Rapid Commun.* **2019**, *40*, 1800207.

[4] a) E. Y. Chernikova, D. V. Berdnikova, *Chem. Commun.* **2020**, *56*, 15360; b) W. Yuan, J. Ma, Z. Zhao, S. Liu, *Macromol. Rapid Commun.* **2020**, *41*, 2000022.

[5] Q.i Liu, T.-X. Zhang, Y. Zheng, C. Wang, Z. Kang, Y.u Zhao, J. Chai, H.-B. Li, D.-S. Guo, Y. Liu, L. Shi, *Small* **2021**, *17*, 2006223.

[6] T. Xiao, L. Qi, W. Zhong, C. Lin, R. Wang, L. Wang, *Mater. Chem. Front.* **2019**, *3*, 1973.

[7] G.-Z. Yin, W.-B. Zhang, S. Z. D. Cheng, *Sci. China Chem.* **2017**, *60*, 338.

[8] a) W.-C. Geng, Q. Huang, Z. Xu, R. Wang, D.-S. Guo, *Theranostics* **2019**, *9*, 3094; b) J. L. Jiménez Blanco, J. M. Benito, C. Ortiz Mellet, J. M. García Fernández, *J. Drug Delivery Sci. Technol.* **2017**, *42*, 18.

[9] M. González-Cuesta, C. Ortiz Mellet, J. M. García Fernández, *Chem. Commun.* **2020**, *56*, 5207.

[10] a) P. Evenou, J. Rossignol, G. Pembouong, A. Gothland, D. Colesnic, R. Barbeyron, S. Rudiuk, A.-G. Marcelin, M. Ménand, D. Baigl, V.

Calvez, L. Bouteiller, M. Sollogoub, *Angew. Chem., Int. Ed.* **2018**, *57*, 7753; b) L. Gallego-Yerga, M. J. González-Álvarez, N. Mayordomo, F. Santoyo-González, J. M. Benito, C. Ortiz Mellet, F. Mendicuti, J. M. García Fernández, *Chem. - Eur. J.* **2015**, *21*, 12093; c) L. Gallego-Yerga, M. J. González-Álvarez, N. Mayordomo, F. Santoyo-González, J. M. Benito, C. Ortiz Mellet, F. Mendicuti, J. M. García Fernández, *Chem. - Eur. J.* **2014**, *20*, 6622.

[11] a) L. Gallego-Yerga, J. M. Benito, L. Blanco-Fernández, M. Martínez-Negro, I. Vélaz, E. Aicart, E. Junquera, C. Ortiz Mellet, C. Tros De Ilarduya, J. M. García Fernández, *Chem. - Eur. J.* **2018**, *24*, 3825; b) A. I. Carbajo-Gordillo, J. Rodríguez-Lavado, J. L. Jiménez Blanco, J. M. Benito, C. Di Giorgio, I. Vélaz, C. Tros de Ilarduya, C. Ortiz Mellet, J. M. García Fernández, *Chem. Commun.* **2019**, *55*, 8227; c) T. Neva, A. I. Carbajo-Gordillo, J. M. Benito, H. Lana, G. Marcelo, C. Ortiz Mellet, C. Tros De Ilarduya, F. Mendicuti, J. M. García Fernández, *Chem. - Eur. J.* **2020**, *26*, 15259.

[12] A. I. Carbajo-Gordillo, M. González-Cuesta, J. L. Jiménez Blanco, J. M. Benito, M. L. Santana-Armas, T. Carmona, C. Di Giorgio, C. Przybylski, C. Ortiz Mellet, C. Tros De Ilarduya, F. Mendicuti, J. M. García Fernández, *Chem. - Eur. J.* **2021**, *27*, 9429.

[13] A. I. Carbajo-Gordillo, J. L. Jiménez Blanco, J. M. Benito, H. Lana, G. Marcelo, C. Di Giorgio, C. Przybylski, H. Hinou, V. Ceña, C. Ortiz Mellet, F. Mendicuti, C. Tros De Ilarduya, J. M. García Fernández, *Biomacromolecules* **2020**, *21*, 5173.

[14] a) S. Srinivasachari, K. M. Fichter, T. M. Reineke, T. M. Reineke, *J. Am. Chem. Soc.* **2008**, *130*, 4618; b) Á. Martínez, C. Bienvenu, J. L. Jiménez Blanco, P. Vierling, C. Ortiz Mellet, J. M. García Fernández, C. Di Giorgio, *J. Org. Chem.* **2013**, *78*, 8143.

[15] a) C. Barner-Kowollik, F. E. Du Prez, P. Espeel, C. J. Hawker, T. Junkers, H. Schlaad, W. Van Camp, *Angew. Chem., Int. Ed.* **2011**, *50*, 60; b) L. Gallego-Yerga, C. De La Torre, F. Sansone, A. Casnati, C. Ortiz Mellet, J. M. García Fernández, V. Ceña, *Carbohydr. Polym.* **2021**, *252*, 117135.

[16] J. M. Benito, J. L. Jiménez Blanco, C. Ortiz Mellet, J. M. García Fernández, *Angew. Chem., Int. Ed.* **2002**, *41*, 3674.

[17] S. Shao, Q. Zhou, J. Si, J. Tang, X. Liu, M. Wang, J. Gao, K. Wang, R. Xu, Y. Shen, *Nat. Biomed. Eng.* **2017**, *1*, 745.

[18] P. Terrier, J. Tortajada, G. Zin, W. Buchmann, *J. Am. Soc. Mass Spectrom.* **2007**, *18*, 1977.

[19] C. M. Maguire, M. Rösslein, P. Wick, A. Prina-Mello, *Sci. Technol. Adv. Mater.* **2018**, *19*, 732.

[20] N. Smiljanic, V. Moreau, D. Yockot, J. M. Benito, J. M. García Fernández, F. Djedaïni-Pilard, *Angew. Chem., Int. Ed.* **2006**, *45*, 5465.

[21] G. Grandinetti, A. E. Smith, T. M. Reineke, *Mol. Pharmaceutics* **2012**, *9*, 523.

[22] T. Haraguchi, T. Koujin, T. Shindo, Ş. Bilir, H. Osakada, K. Nishimura, Y. Hirano, H. Asakawa, C. Mori, S. Kobayashi, Y. Okada, Y. Chikashige, T. Fukagawa, S. Shibata, Y. Hiraoka, *Commun. Biol.* **2022**, *5*, 78.

[23] H. Bai, G. M. S. Lester, L. C. Petishnok, D. A. Dean, *Biosci. Rep.* **2017**, *37*, BSR20160616.

[24] D. Rodríguez-Lucena, J. M. Benito, E. Álvarez, C. Jaime, J. Perez-Miron, C. Ortiz Mellet, J. M. García Fernández, *J. Org. Chem.* **2008**, *73*, 2967.

[25] a) V. Villari, A. Mazzaglia, R. Darcy, C. M. O'Driscoll, N. Micali, *Biomacromolecules* **2013**, *14*, 811; b) L. Gallego-Yerga, M. Lomazzi, V. Franceschi, F. Sansone, C. Ortiz Mellet, G. Donofrio, A. Casnati, J. M. García Fernández, *Org. Biomol. Chem.* **2015**, *13*, 1708.

[26] K. Fant, E. K. Esbjörner, P. Lincoln, B. Nordén, *Biochemistry* **2008**, *47*, 1732.

[27] C. Chittimalla, L. Zammut-Italiano, G. Zuber, J.-P. Behr, *J. Am. Chem. Soc.* **2005**, *127*, 11436.

[28] a) L. M. Kranz, M. Diken, H. Haas, S. Kreiter, C. Loquai, K. C. Reuter, M. Meng, D. Fritz, F. Vascotto, H. Hefesha, C. Grunwitz, M. Vormehr, Y. Hüsemann, A. Selmi, A. N. Kuhn, J. Buck, E. Derhovanessian, R. Rae, S. Attig, J. Diekmann, R. A. Jabulowsky, S. Heesch, J. Hassel, P. Langguth, S. Grabbe, C. Huber, Ö. Türeci, U. Sahin, *Nature* **2016**, *534*, 396; b) Q. Cheng, T. Wei, L. Farbiak, L. T. Johnson, S. A. Dilliard, D. J. Siegwart, *Nat. Nanotechnol.* **2020**, *15*, 313.